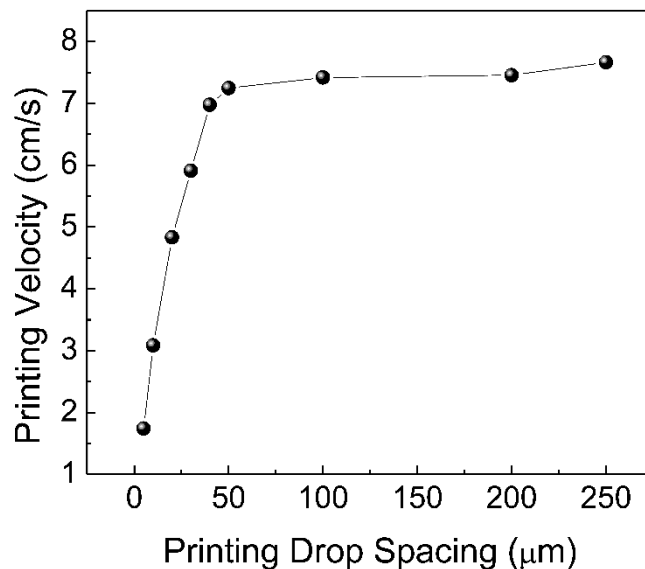
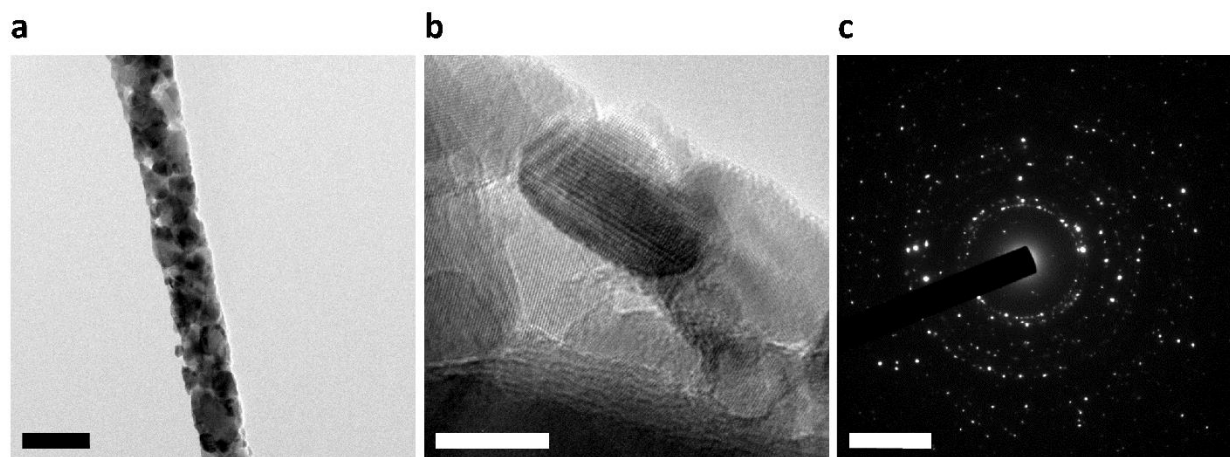


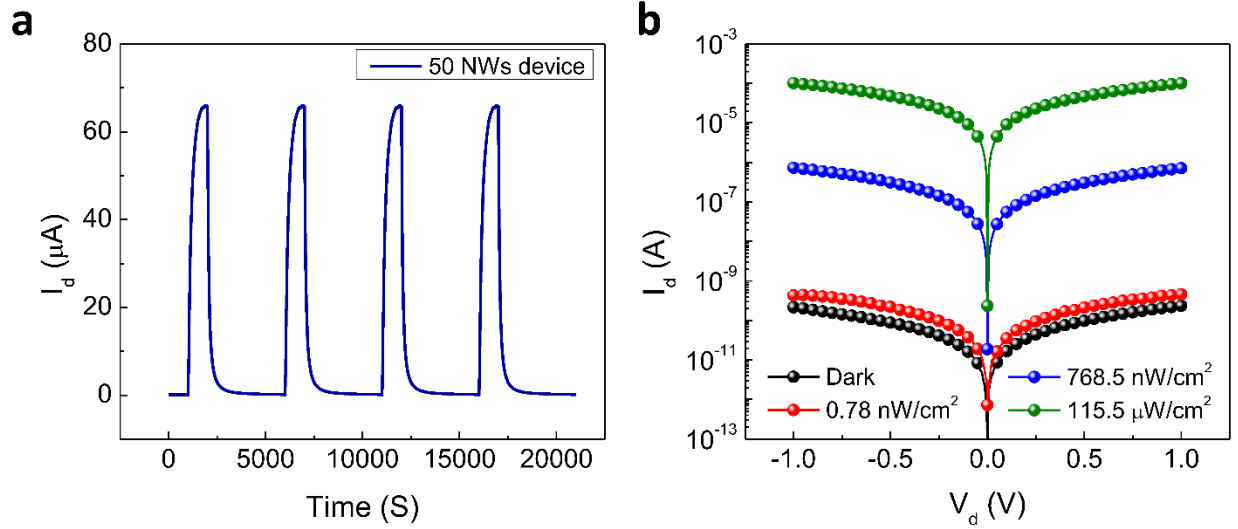
**Supplementary Figure 1. Different GNW printing spacing and XRD characterization.** (a, b) Optical images of the as-printed electrospun ZnO nanofibers with spacing of 20 and 30 μm, respectively. Scale bars, 100 μm. (c) X-ray diffraction patterns of the as-printed and as-calcinated ZnO GNWs.



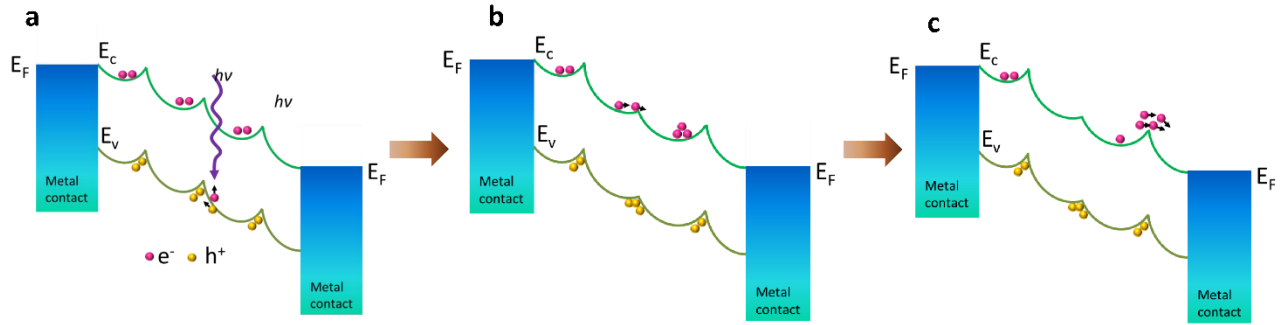
**Supplementary Figure 2.** Printing velocity vs. drop spacing of Dimatrix Materials Printer. Printing head translation velocity for Dimatrix materials printer is controlled by selecting drop spacing. More specifically, the function of printing a horizontal line is realized by virtually dropping ink dot by dot along the X direction (Figure 1a) when the printing head is moving. The action of dropping ink takes milliseconds at each dot. In this work, 5 μm, 10 μm, 20 μm and 30 μm drop spacing have been chosen to print nanofibers with tunable spacing. The printing head translation velocity versus the drop spacing is shown in Supplementary Figure 2 above, in which the average velocity is  $1.74\text{cm}\cdot\text{s}^{-1}$ ,  $2.09\text{cm}\cdot\text{s}^{-1}$ ,  $4.83\text{cm}\cdot\text{s}^{-1}$  and  $5.91\text{cm}\cdot\text{s}^{-1}$ , respectively. It was reported that if the nanofibers electrospinning speed is much faster than the fiber collection substrate translation velocity, the “local spiraling” will occur<sup>14</sup>. In this work, it can be seen from Figure 1d (5 μm line spacing), Figure 1e (10 μm), Supplementary Figure 1a (20 μm) and 1b (30 μm) that most of the nanofibers are straight which indicates reasonable velocity matching between electrospinning and printing. However, there are more local spirals in Figure 1d (5 μm line spacing) than other cases where line spacing is larger due to relatively slower printing head velocity for 5 μm line spacing printing.



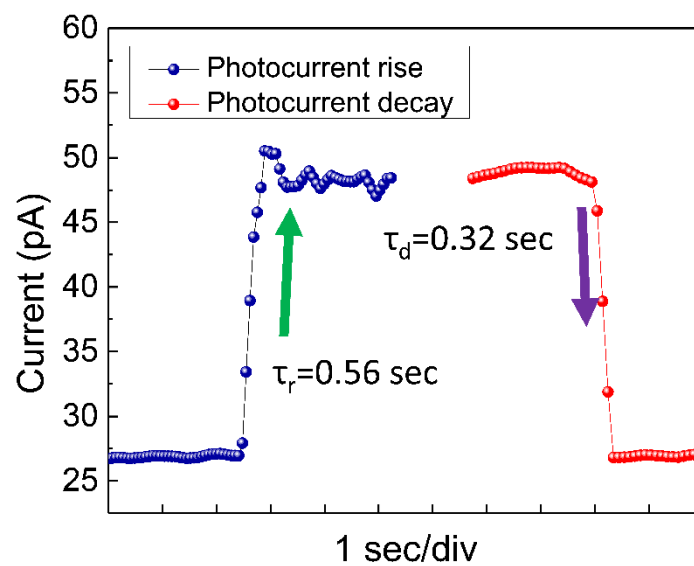
**Supplementary Figure 3. GNW TEM characterization.** (a) TEM image of as-calcinated ZnO GNW. Scale bar, 100 nm. (b) Magnified TEM image to show the grains inside the GNWs. Scale bar, 10 nm. (c) Electron diffraction pattern of GNW. Scale bar, 51 /nm.



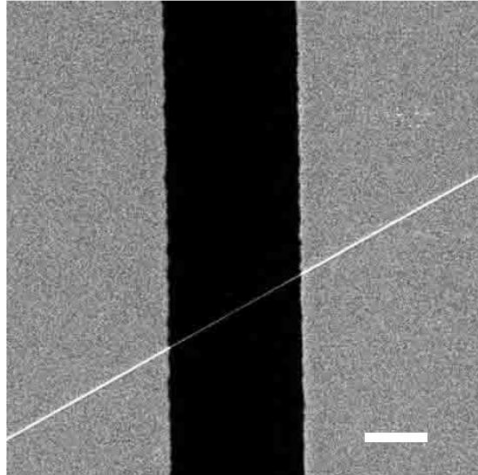
**Supplementary Figure 4. Photoresponse of the printed ZnO GNWs photodetectors with 50 NWs.** (a) Time domain photoresponse of the printed ZnO GNWs photodetector under UV irradiance of  $77.5 \mu\text{W}\cdot\text{cm}^{-2}$  at +1V bias voltage. (b)  $I$ - $V$  curves of the printed ZnO GNWs photodetector at dark,  $0.5 \text{ nW}\cdot\text{cm}^{-2}$ ,  $768.5 \text{ nW}\cdot\text{cm}^{-2}$ , and  $115.5 \mu\text{W}\cdot\text{cm}^{-2}$  of UV illumination at +1V biased voltage.



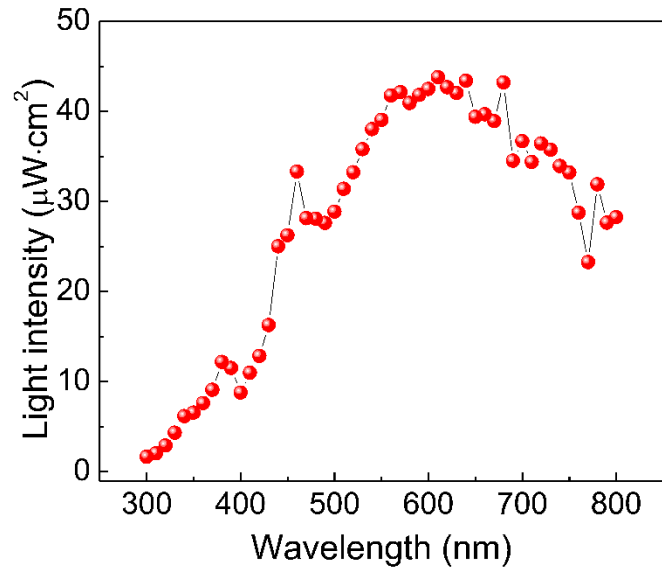
**Supplementary Figure 5.** Schematic of the Schottky barrier height modulation mechanism and carrier multiplication process for extremely low photon flux down to  $\sim 12$  photons absorbed per sec for the GNW device. **(a)** Multiple barriers along the GNW axial direction. **(b)** One barrier lowering event triggered by photon absorption. **(c)** Carrier multiplication and transport driven by the external field.



**Supplementary Figure 6.** Rise and decay of photocurrent responding to switching on and off of  $0.5 \text{ nW} \cdot \text{cm}^{-2}$  UV intensity.



**Supplementary Figure 7.** An individual single-crystal CVD grown ZnO NW device fabricated by contact printing, followed by photolithography and metal evaporation (Ti/Au :10/90nm). Scale bar, 1  $\mu$ m.



**Supplementary Figure 8.** The output spectrum of the quantum efficiency system used for the photoconduction spectra measurements.